JOURNAL OF GEOPHYSICAL RESEARCH, VOL. 112, D06313, doi:10.1029/2006JD007339, 2007

A stratospheric ozone profile data set for 1979–2005: Variability, trends, and comparisons with column ozone data

William J. Randel[1] and Fei Wu[1]

Received 23 March 2006; revised 10 July 2006; accepted 22 November 2006; published 31 March 2007.

[1] A global stratospheric ozone data set for 1979–2005 is described. Interannual variations are derived from analysis of Stratospheric Aerosol and Gas Experiment (SAGE I and II) profile measurements, combined with polar ozonesonde data from Syowa (69°S) and Resolute (75°N). These interannual changes are combined with a seasonally varying ozone climatology from Fortuin and Kelder [1998] to provide a monthly global data set. These data are intended for use in global modeling studies and for analysis of global variability and trends. In order to generate continuous fields from the gappy SAGE data, we use a regression fit that includes decadal trends, solar cycle, and QBO terms, and the spatial structure of these variations is studied in detail. Decadal trends are modeled using an equivalent effective stratospheric chlorine proxy. Ozone variability from the vertically integrated SAGE/sonde data set is compared with results derived from a merged Total Ozone Mapping Spectrometer/solar backscatter ultraviolet column ozone data set, showing good overall agreement (in particular for trends in extratropics). We also compare the SAGE data with ozonesonde measurements over Northern Hemisphere midlatitudes and find excellent agreement for lower stratospheric variability and trends. In the tropics, the SAGE ozone data show relatively large percentage decreases in the lower stratosphere. However, the vertically integrated SAGE data do not agree with column ozone trends in the tropics, so there is less confidence in the SAGE results in this region.

Citation: Randel, W. J., and F. Wu (2007), A stratospheric ozone profile data set for 1979–2005: Variability, trends, and comparisons with column ozone data, *J. Geophys. Res.*, *112*, D06313, doi:10.1029/2006JD007339.

1. Introduction

[2] The effects of stratospheric ozone variability and change are important for modeling and attribution of global change. The studies of *Santer et al.* [1996] and *Bengtsson et al.* [1999] demonstrate that stratospheric ozone change is a crucial ingredient for modeling the detailed vertical structure of temperature changes in the troposphere and stratosphere. Modeling studies also confirm that ozone loss is a dominant mechanism leading to cooling of the lower stratosphere since ~1980 [*Langematz et al.*, 2003; *Shine et al.*, 2003; *Dameris et al.*, 2005; *Ramaswamy et al.*, 2006]. In order to accurately model and assess the impacts of stratospheric ozone variability and change, it is important to have detailed knowledge of past behavior, in particular for the vertical profile of ozone. To that end, we present here a global ozone profile data set for the stratosphere that covers the time period 1979–2005.

[3] The ozone profile data set described here results from combining a seasonally varying ozone climatology [from *Fortuin and Kelder*, 1998] with interannual changes derived from global measurements spanning 1979–2005. Interannual variability in ozone profile data is derived over the majority of the globe using Stratospheric Aerosol and Gas Experiment (SAGE) I and II measurements [*McCormick et al.*, 1989]. These data have the key attributes of long-term accuracy plus high vertical resolution. The SAGE data primarily cover the latitude range ~ 55°N–5°S (depending on month). Because polar regions are not observed during most of the year by SAGE, we use ozone profile measurements from ozonesondes at Syowa (69°S) and Resolute (75°N), which have reasonably complete records over 1979–2005 up to ~27 km. Upper stratospheric polar regions are extrapolated from high-latitude SAGE I and II data.

[4] Beyond simply generating a continuous global data set, we include an updated analysis of interannual variability observed in the ozone profile data, in particular examining the spatial structure of long-term decadal trends, solar cycle variability, and quasi-biennial oscillation (QBO) effects. These components contribute a majority of interannual variability in both profile and column ozone, and our results provide an updated analysis based on SAGE I and II data [cf. *Wang et al.*, 1996, 2002; *Randel and Wu*, 1999; *Li et al.*, 2002; *World Meteorological Organization (WMO)*, 2003]. A further focus is to make detailed comparisons between the vertically integrated profile data and global column ozone data derived from merged Total Ozone Mapping

[1]National Center for Atmospheric Research, Boulder, Colorado, USA.

0148-0227/07/2006JD007339$09.00

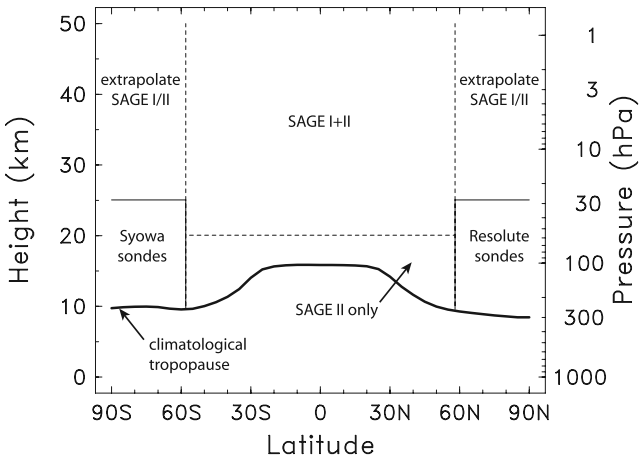

Figure 1. Schematic diagram showing data sources used to calculate interannual variability for the global ozone profile data set.

Spectrometer/solar backscatter ultraviolet (TOMS/SBUV) measurements [*Stolarski et al.*, 2006]. These comparisons include analysis of both time series and the statistical fits of trends and solar cycle variability. While there is good overall agreement between the integrated profile and column ozone data sets, we highlight differences that point to uncertainties in current understanding of low-frequency ozone variability and trends. We also include comparisons between the SAGE ozone profile data and ozonesonde measurements over Northern Hemisphere (NH) midlatitudes, in order to improve understanding of SAGE-derived results in the lower stratosphere.

2. Data and Analyses

2.1. SAGE/Sonde Data Set

[5] Accurate estimates of interannual variability and trends are derived using ozone measurements from the SAGE I and SAGE II satellites over most of the globe (55°N-S), together with ozonesonde profile measurements over both polar regions. The merging of the data sets is shown schematically in Figure 1. The domain is global, covering altitudes from the climatological tropopause (derived from NCEP reanalysis) to 50 km, with a spatial sampling of 5° latitude and 1 km.

[6] Results over 55°N–S are derived from SAGE I and II data [*McCormick et al.*, 1989]. SAGE I data span the time period 1979–1981, and cover an altitude range of 20–50 km. SAGE I data employ the altitude registration adjustments recommended by *Wang et al.* [1996]. SAGE II data cover the time period November 1984 to August 2005 (when the satellite ceased operation), and span a wider altitude range from the tropopause to 50 km. The SAGE II data used here are based on the v6.2 retrieval algorithm. Data are omitted for 2 years following the eruption of Pinatubo in June 1991, when high levels of stratospheric aerosols influenced the SAGE retrievals [*Wang et al.*, 2002]. The SAGE I and II solar occultation measurements cover much of the latitude range 55°N–S during approximately one month, but there are substantial gaps in monthly sampled data at individual latitudes [see *McCormick et al.*, 1989, Figure 1]. Both sunrise and sunset SAGE II data are used as available; only sunset measurements are available after mid-2000. Because of irregular data gaps, we use a regression analysis (discussed below) to generate a continuous data set; although there is substantial sampling uncertainty for individual months from SAGE, the data are probably adequate for quantifying low-frequency interannual variability (as demonstrated in our comparisons with column ozone data and ozonesondes). Although the SAGE II data end in August 2005, for completeness we extend our results to the end of 2005 (based on extended time series of proxy variables).

[7] Ozone profile data in the polar regions (poleward of 60° latitude) are based on monthly sampled ozonesonde measurements from two stations with relatively continuous time series: Syowa (69°S) and Resolute (75°N). These data were obtained from the World Ozone and Ultraviolet Radiation Data Center (WOUDC), from the Web site http://www.woudc.org/. We use the polar ozonesonde data for altitudes from the tropopause to 30 hPa; above this level the polar results are based on extrapolation of the SAGE I and II data.

[8] We use a regression analysis to generate a continuous interannual anomaly data set from the combined SAGE I and II and polar ozonesonde data sets. Each data set is first deseasonalized using a harmonic regression of monthly binned data, and ozone anomalies at each latitude and height are fit with a regression model of the form

$$O_Z(t) = \alpha \bullet \text{decadal trend} + \beta \bullet \text{solar cycle} + \gamma_1 \bullet \text{QBO}_1 + \gamma_2 \bullet \text{QBO}_2 \quad (1)$$

Decadal trend changes in ozone are modeled using the equivalent effective stratospheric chlorine (EESC) proxy shown in Figure 2a [*WMO*, 2003; *Fioletov and Shepherd*, 2005; *Stolarski et al.*, 2006]. This term is intended to isolate ozone changes associated with the amount of ozone-depleting chlorine and bromine in the stratosphere. The EESC function used here has a maximum in 1997, and is most appropriate for midlatitude ozone (EESC probably peaks later in polar regions, associated with older stratospheric age of air, but this variability will not strongly influence our trend results). The solar cycle proxy is the standard $F_{10.7}$ radio flux (Figure 2b), and QBO_1 and QBO_2 are two orthogonal QBO time series based on observed equatorial stratospheric winds [*Wallace et al.*, 1993; *Randel and Wu*, 1996]. We include a constant plus annual harmonic term for each of the regression coefficients in equation (1). Figure 3a shows an example of the regression fit to SAGE I and II ozone measurements at one particular latitude and height (40°N, 21 km). The regression analysis provides a reasonable overall fit of the monthly data, and the data in Figure 3a show a clear decadal-scale decrease in ozone, in addition to relatively large QBO variability. Overall the regression fits explain a large fraction (~50–70%) of the interannual variance in the monthly SAGE data over much of the stratosphere, as shown in Figure 3b. The regression model captures a relatively low fraction of interannual variance in the extratropical lower stratosphere (below 20 km) in Figure 3b, although the overall variance of the SAGE data is large in this region. This is probably due to

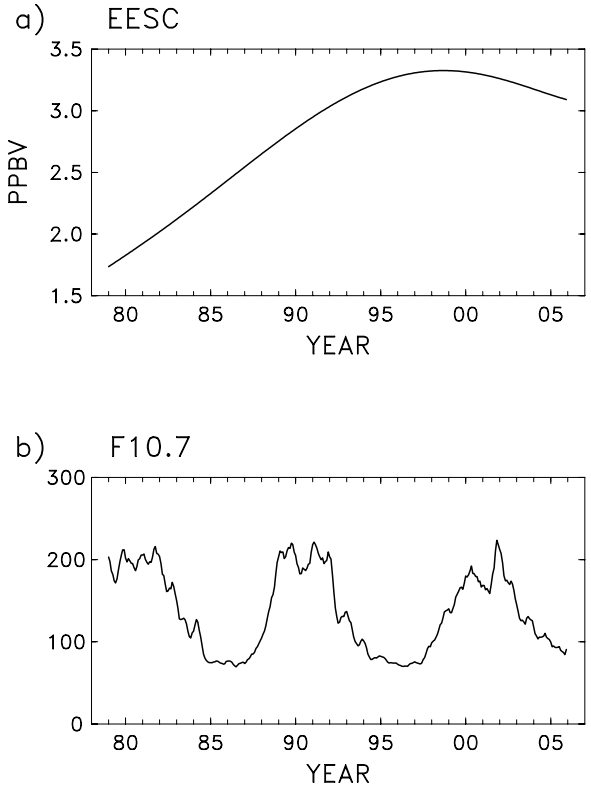

Figure 2. (a) Time series of equivalent effective stratospheric chlorine (EESC), used as a proxy for decadal trend variations in ozone. (b) Time series of smoothed solar $F_{10.7}$ radio flux, used as a proxy for solar cycle variations in ozone.

large month-to-month meteorological variability of ozone in this region [e.g., *Newchurch et al.*, 2003] which is not captured in the regression analysis.

[9] A further detail in the data analysis is that SAGE I data are unavailable below 20 km, so that the 1979–2005 regression results for altitudes from the tropopause to 20 km are based solely on SAGE II measurements for 1984–2005. While the resulting decadal trend and QBO fits are reasonably continuous across 20 km, the solar cycle fit changes sign (with negative projection below 20 km). Because this seems to be an artifact related to data details, we omit the solar cycle term in the regressions below 20 km. Note that we do not include a volcanic aerosol proxy term in our statistical analysis (as in work by *Stolarski et al.* [2006]), because there are no SAGE data available for postvolcanic periods (the eruption of El Chichon (April 1982) occurred during the SAGE I and II data gap, and SAGE II data are unavailable after the eruption of Mt. Pinatubo in June 1991, as discussed above).

[10] The regression fits are handled somewhat differently for the polar ozonesonde data. Because of large year-to-year variability in polar regions (especially for single station measurements), we find that the solar and QBO regression fits give unphysical results (such as strong oscillations in the vertical). Hence only the decadal trend (EESC) fits are used for the polar data (and solar and QBO fits are only analyzed over 55°N–S). The ozonesonde trends are assigned to latitudes 65°–90° (constant values), and the SAGE I and II and ozonesonde data are merged by interpolation over latitudes 55°–65°N and S to provide a smooth, continuous data set.

2.2. Merged TOMS/SBUV Column Ozone Data

[11] Part of the analysis here includes comparisons between the vertically integrated ozone profile data set and global satellite column ozone data. The column ozone data here are from the merged satellite column ozone data discussed by *Stolarski et al.* [2006], based on monthly means covering 1979–2005. These merged data are derived from a combination of TOMS and SBUV measurements, and are based on the v8 retrieval algorithm. These data were obtained from the merged data Web site (http://code916.gsfc.nasa.gov/Data_services/merged/), and details of the data construction can be found there. Regression results for the column ozone data are calculated omitting two years of data after the El Chichon (April 1982) and Mt. Pinatubo (June 1991) volcanic eruptions.

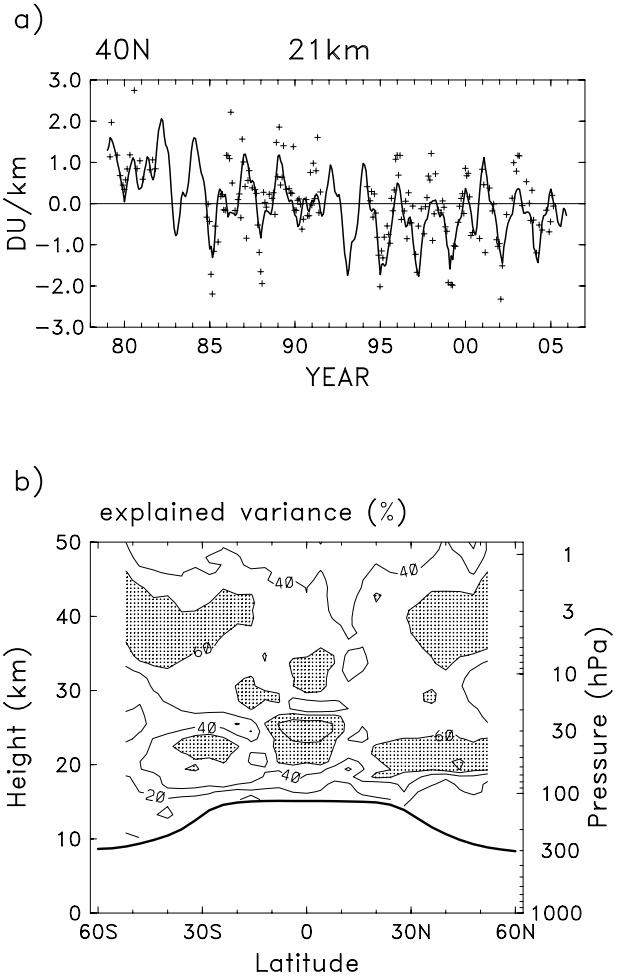

Figure 3. (a) Time series of monthly binned, deseasonalized ozone observations from SAGE I and II at 40°N and 21 km (pluses), together with the regression fit at this location based on trend, solar cycle, and QBO variations. Note the gaps in the observations during 1982–1984 and 1991–1993. (b) Contour plot of the fraction of interannual variance explained in SAGE I and II data by the regression model. Contours are 20%, 40%, 60%, and 80%.

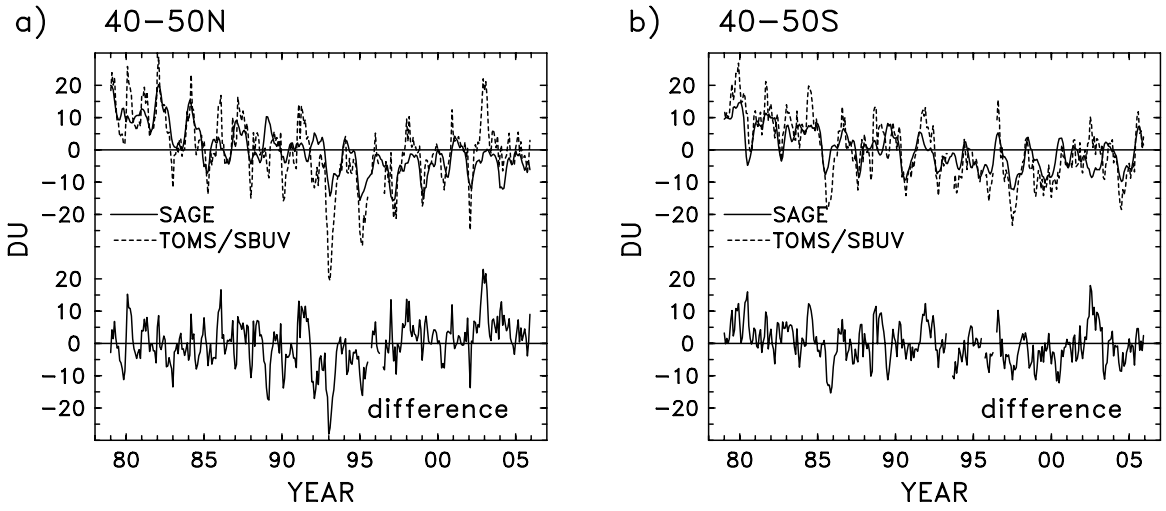

Figure 4. Time series of deseasonalized column ozone anomalies from vertically integrated SAGE I and II data (using regression fits, as in Figure 3) compared with column ozone from merged TOMS/SBUV data (top curves). Results are shown for data over (a) 40°–50°N and (b) 40°–50°S. The bottom curves show the respective difference time series.

2.3. NH Midlatitude Ozonesondes

[12] We also include comparisons of ozone profile variability between the SAGE data and ozonesonde measurements in the lower stratosphere over NH midlatitudes, where there are several stations with relatively long and continuous time series [e.g., *Logan et al.*, 1999]. The ozonesonde data analyzed here include measurements from stations in Japan (Sapporo, Tateno, and Kagoshima), Europe (Hohenpeissenberg, Payerne, Lindenberg, and Uccle), and North America (Boulder, Wallops Island, Churchill, Edmonton and Goose Bay), and were obtained from the WOUDC. These stations cover the latitude range 32°–53°N. In order to obtain an estimate of interannual variability over midlatitudes most representative of the (zonal mean) SAGE data, the ozonesonde data have been deseasonalized at each station, and the anomalies averaged over the available stations for each month at each pressure level. These averaged data are then compared to SAGE results averaged over 35°–55°N.

3. Results

3.1. Comparison of Time Series With Column Ozone Data

[13] It is useful to compare interannual variability in the vertically integrated profile data with that observed in global column ozone data sets. Here we compare deseasonalized anomalies in the monthly SAGE/sonde data set, vertically integrated from the tropopause to 50 km, with deseasonalized anomalies derived from the merged TOMS/SBUV satellite column ozone data. Note that the deseasonalized column ozone data contain the full observed month-to-month variability, whereas the integrated SAGE/sonde data contain only components associated with trends, solar and QBO variability.

[14] Figure 4 compares the time series of vertically integrated profile anomalies with column ozone anomalies for latitudes 40°–50°N and 40°–50°S, together with their respective differences. Overall there is reasonable agreement in the anomaly time series, with the main components of variability associated with decadal-scale decreases and QBO fluctuations. Monthly differences are typically of order ±10 DU. There are somewhat larger differences observed over 40°–50° N for ~1992–1995, when the TOMS/SBUV column measurements are lower than the integrated SAGE data. This period follows the Mt. Pinatubo volcanic eruption in 1991, and ozone decreases for this period have been attributed to chemical [*Tie et al.*, 1994] and/or dynamical effects [*Hadjinicolaou et al.*, 1997]. As discussed above, such volcanic effects are not included in our regression analysis. Besides this period, the differences in Figure 4 do not show obvious systematic patterns, but

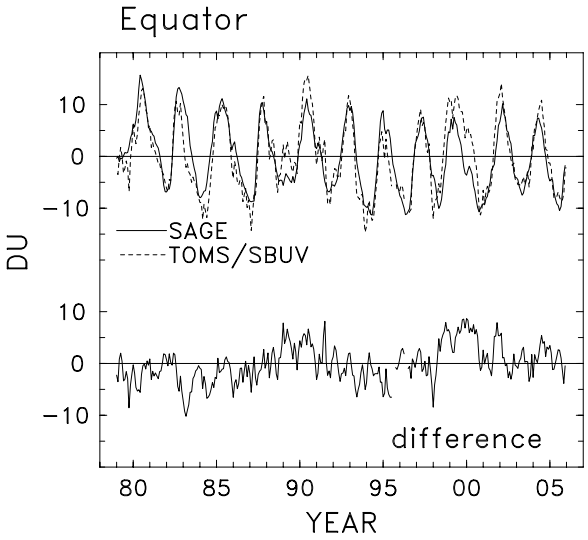

Figure 5. Time series of deseasonalized column ozone anomalies at the equator, derived from vertically integrated SAGE I and II data and merged TOMS/SBUV measurements (top curve). Bottom curve shows the difference time series.

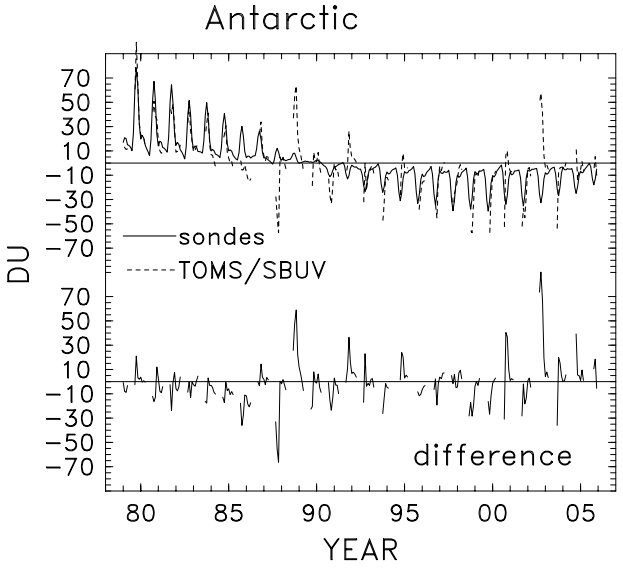

Figure 6. Time series of deseasonalized column ozone anomalies over the Antarctic (70°S), derived from vertically integrated ozonesonde measurements (from Syowa) and merged TOMS/SBUV data. Note that the TOMS/SBUV measurements are unavailable during polar night. The bottom curve shows the difference time series.

probably reflect month-to-month meteorological variability (not captured by our regression analysis of SAGE I and II data).

[15] Figure 5 compares equatorial variations in column ozone from the two data sets. Here the QBO is the dominant component of variability, and there is excellent agreement in amplitude and phase of the QBO variations, demonstrating that SAGE measurements accurately resolve the QBO vertical structure [e.g., *Randel and Wu*, 1996]. The equatorial difference time series in Figure 5 shows somewhat larger differences during ~1989–1991 and ~1998–2001 (integrated SAGE lower than the column measurements). These periods correspond to solar maximum conditions (Figure 2b), and correspondingly there is a significant difference in the equatorial solar cycle fits between the vertically integrated SAGE and TOMS/SBUV data (as discussed below).

[16] Column ozone variations in the Antarctic region are shown in Figure 6, comparing vertically integrated regression fit of the Syowa ozonesonde data with the merged column ozone data (note the latter are unavailable at 70°S during April–September). While there is good agreement in the decadal-scale changes, there are significant residuals related to year-to-year meteorological variability (such as for 2002). Such interannual meteorological variability is even higher for the Arctic region (not shown here).

[17] Figure 7a quantifies the interannual variance in the integrated profile and merged column ozone data sets as a function of latitude, and Figure 7b shows the correlation between the two data sets over the entire record 1979–2005. Over the latitude range 30°N–S the integrated SAGE data has similar variance to the column measurements, and anomaly correlations are 0.6–0.8. The latitudinal maxima in variance at the equator and ~30°N/S reflect the dominance of the QBO for interannual variability in low latitudes (i.e., Figure 5). Over middle latitudes the column ozone data have significantly more variance than the regressed SAGE data, and this reflects the additional month-to-month meteorological variability seen in Figure 4 (but note that the anomaly correlations are still ~ 0.7). Much of this month-to-month variability in ozone occurs below 20 km [*Newchurch et al.*, 2003], and the extratropical differences in Figure 7a are consistent with the relatively low fractional variance explained by the regression model below 20 km in Figure 3b. The large interannual variance over Antarctica in Figure 7a reflects development of the ozone hole over 1979–2005 (Figure 6). Somewhat lower anomaly correlations over the Arctic reflect a higher level of meteorological variability not captured in the regression analysis.

3.2. Decadal Trends

[18] A meridional cross section of decadal-scale trends in the ozone profile data is shown in Figure 8a. These trends

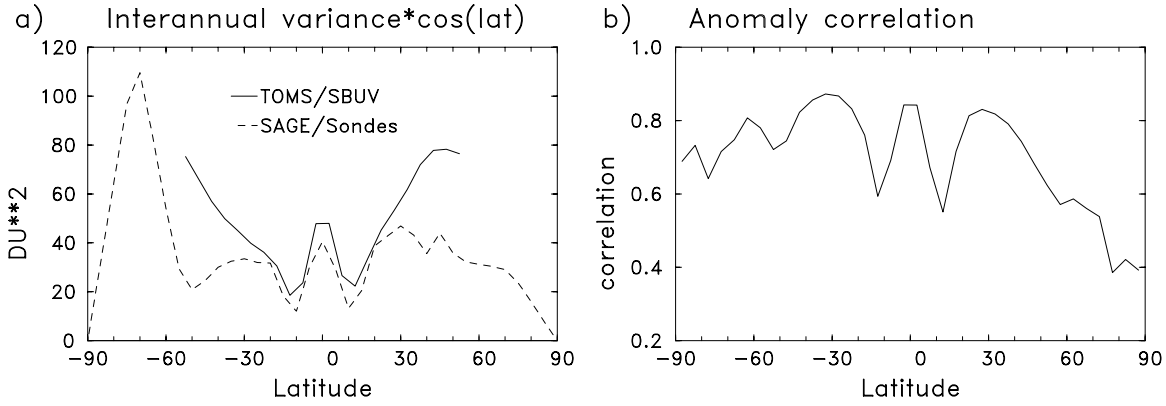

Figure 7. (a) Interannual variance of deseasonalized column ozone anomalies over 1979–2005, derived from the vertically integrated SAGE/sonde data set and merged TOMS/SBUV data. The variance is scaled by cos (latitude), and results for TOMS/SBUV data are only shown over 60°N–S because of lack of polar night data. (b) Correlation between column ozone anomalies from vertically integrated SAGE/sonde data and merged TOMS/SBUV data. For polar regions (>55°), the correlations are only calculated for months when TOMS/SBUV data were available.

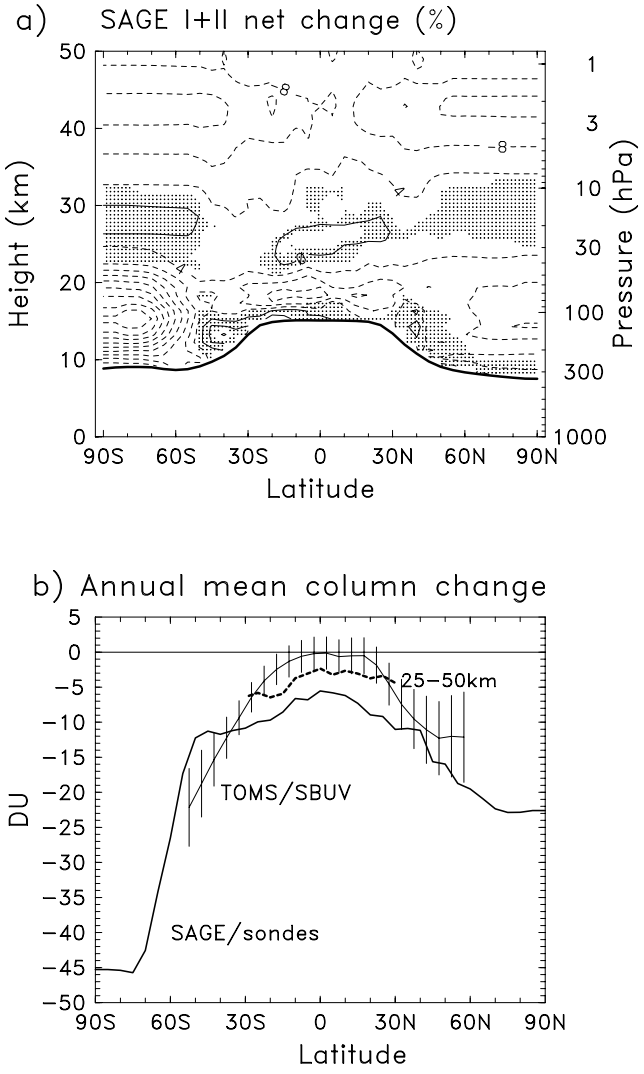

Figure 8. (a) Meridional cross section of decadal trends in the combined SAGE/sonde data set, derived from regression onto EESC (Figure 2a). Trends are expressed in terms of net percentage change during 1979–2005, as described in text. Contours are −4%, −8%, −12%, −16%, −20%, −30%, −40%, and shading denotes that the trends are not statistically significant at the 2*sigma level. (b) Latitudinal structure of annual mean column ozone trends during 1979–2005, derived from vertically integrated SAGE/sonde data and merged TOMS/SBUV data. Error bars on the TOMS/SBUV curve denote 2*sigma statistical uncertainty levels. Trends are expressed in terms of net ozone change over 1979–2005. The thick dashed line denotes trends derived from SAGE data, integrated only over 25–50 km.

are derived as a regression onto the EESC time series in Figure 2a, and results can be expressed in several alternative ways.

[19] 1. The results can be simply expressed as ozone change per unit of EESC (say, % per 0.1 ppbv EESC).

[20] 2. The EESC time series is nearly linear for 1979–1989 (see Figure 2a), with a net change of approximately 1.0 ppbv of chlorine. Thus the EESC fit to ozone can be expressed in terms of linear changes for this time period, with results reported in ozone changes per decade (as in the work by *Stolarski et al.* [2006]).

[21] 3. Ozone changes associated with EESC can also be expressed as simple differences between two time periods. Here we show results expressed as the total change in ozone between 1979 and 2005; these values work out to be approximately 1.4 times the linear decadal trend values for 1979–1989 discussed in result 2 above (i.e., a −5% per decade trend corresponds to a $\sim -7\%$ change for 1979–2005). We choose this expression because it provides a simple measure of the net ozone changes during the 1979–2005 observational record.

[22] The ozone profile decadal changes in Figure 8a show the familiar pattern of maxima in the upper stratosphere (∼35–45 km) and lower stratosphere (∼15–25 km), and minimum near 30 km, seen in previous analyses [e.g., *Stratospheric Processes and their Role in Climate*, 1998; *Wang et al.*, 2002; *WMO*, 2003]. The upper stratospheric changes show a symmetric latitudinal structure, with net ozone changes of $\sim -12\%$ over middle and high latitudes, and somewhat smaller changes in the tropics (∼−8%). This altitude and latitude structure is a fingerprint of gas phase chlorine-induced ozone loss [*WMO*, 2003]. The seasonal variation of upper stratosphere trends over extratropics shows somewhat larger trends during winter in the NH and autumn-winter in the Southern Hemisphere (not shown), consistent with the results derived from SBUV data (and 2D chemical model results) by *Rosenfield et al.* [2005].

[23] The lower stratosphere trends in Figure 8a show statistically significant changes over all latitudes covered by SAGE measurements ($\sim 55°$N–S). The detailed vertical structure of trends in the lower stratosphere in Figure 8a should be viewed cautiously, because of the details of data availability: SAGE I and II data (1979–2005) are used at and above 20 km, while SAGE II data alone (1984–2000) are used below 20 km. The net changes in ozone near 20 km are of order $\sim -6\%$ over midlatitudes, and somewhat larger in the tropics (∼−10%); these tropical changes are discussed in more detail below. The annual mean polar ozone changes work out to be $\sim -10\%$ in the Arctic and $\sim -40\%$ in the Antarctic, but these changes are strongly seasonally dependent (see below).

[24] The vertical integral of the annual mean global profile trends is shown in Figure 8b, with trends integrated from the local tropopause to 50 km, and expressed in terms of net changes over 1979–2005 (in Dobson units, DU). These are compared with results from the merged column ozone data (with annual mean results over 60°N–S), and these latter include statistical uncertainty estimates. There is reasonable agreement in trends over the midlatitudes of both hemispheres ($\sim 30°-60°$ N and S), while in the tropics the integrated SAGE trends are significantly larger that the column ozone trends (which are near zero in the equatorial region). This difference could have several implications:

[25] 1. Both the integrated SAGE and column trends could be correct, and there could be compensating tropical ozone increases below the tropopause that reconcile the two data sets. This would require a net tropical tropospheric increase of ∼6 DU over 1979–2005, which is approximately a net 15% increase of background values. Tropical tropospheric ozone trends for this period are not well

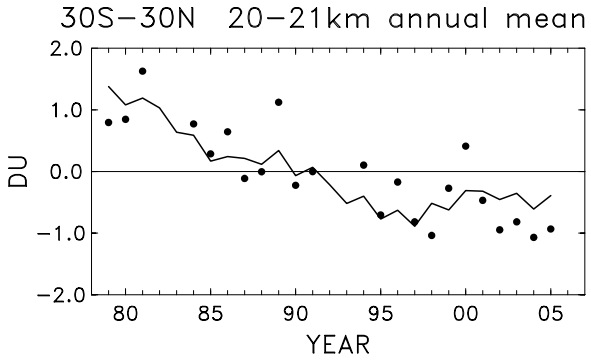

Figure 9. Time series of annual average ozone anomalies over 20–21 km, 30°N-S from SAGE I and II data, plus the regression fit.

known. *Lelieveld et al.* [2004] have reported substantial increases in near-surface ozone in the tropical Atlantic Ocean for 1977–2002, and *Bortz et al.* [2006] suggest a 20% increase in tropical upper tropospheric ozone during 1994–2003 based on aircraft measurements. On the other hand, *Ziemke et al.* [2005] suggest that there have not been significant trends in tropical tropospheric ozone for this period based on satellite observations (specifically, "cloud-slicing" calculations from TOMS data). Given these disparate results and uncertainties, it is difficult to use tropospheric ozone trends as a constraint in evaluating the large tropical differences in Figure 8b.

[26] 2. Another interpretation of the differences is that the integrated SAGE trends are too large in the tropics, in particular in the tropical lower stratosphere. A time series of SAGE I and II data over 20–21 km and 30°N–S is shown in Figure 9, highlighting these tropical changes and the regression fit. The tropical lower stratosphere is a region where satellite measurements are particularly difficult, because of the low ozone density and strong vertical gradients, and there are a number of uncertainties regarding satellite retrievals and aerosol effects. These uncertainties may be crucial for the SAGE I measurements, which anchor the time series at and above 20 km (as seen in Figure 9), and hence have a strong leverage on trend results. Furthermore, decadal trends below 20 km are based only on the shorter time sample from SAGE II alone (1984–2005). As a sensitivity test, Figure 8b includes the tropical SAGE results integrated over a limited vertical range (25–50 km), i.e., neglecting the large lower stratospheric trends seen in Figure 8a. The resulting trends are still larger than the tropical column ozone trends, but the net difference in this case is only ~3 DU.

[27] The latitude-month variations of column ozone trends (expressed as net changes for 1979–2005) are shown in Figure 10, for both the integrated SAGE/sonde data and the merged TOMS/SBUV data. The largest seasonal variations are observed in polar regions, where maximum losses are observed in springtime of both hemispheres. There is reasonable agreement between the integrated sondes and column ozone data in polar regions, subject to the caveat that TOMS/SBUV do not observe polar night (about half of the year). There is also reasonable agreement between the data sets over midlatitudes, although the seasonal variations derived from SAGE (via the harmonic terms incorporated in equation (1) are somewhat different than results from TOMS/SBUV. We note that the detailed SAGE results at latitudes higher than ~30° are sensitive to the SAGE data sampling, which includes regular gaps for certain months. In the tropics both data sets exhibit a similar seasonal cycle for trends (smaller trends during NH winter), but with an offset of approximately 6 DU (larger trends in integrated SAGE data, as discussed above).

3.3. Comparison With NH Midlatitude Ozonesondes

[28] There is a substantial record of ozone profile measurements over the NH midlatitude lower stratosphere available from ozonesondes [e.g., *Logan et al.*, 1999], and these data allow some comparisons to the SAGE-based data set

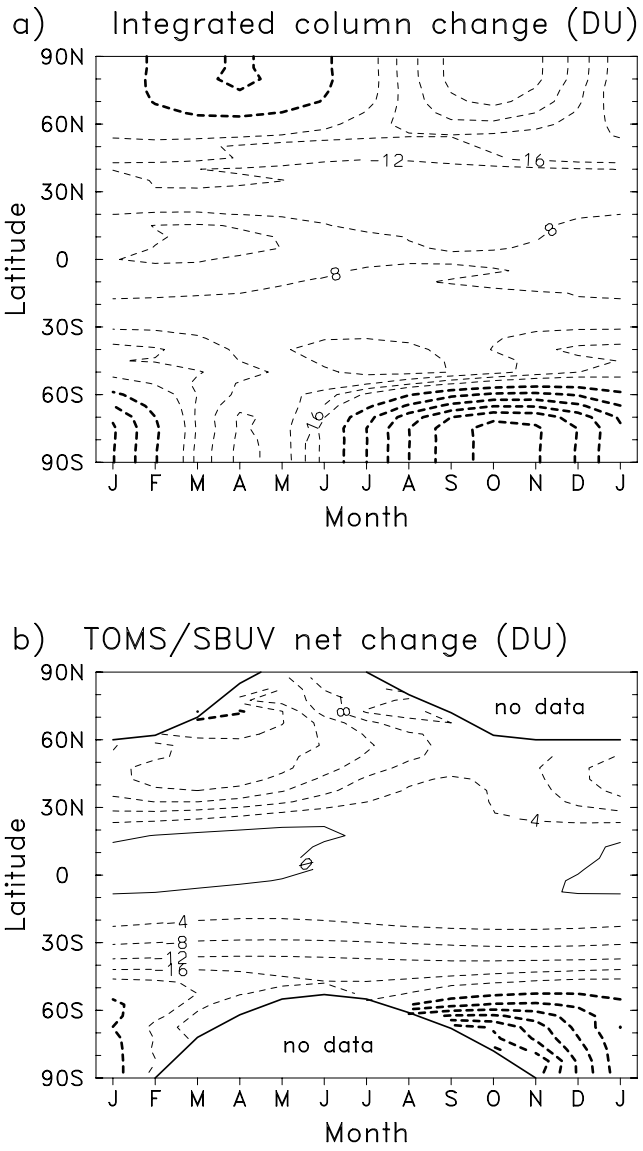

Figure 10. Latitude-time variations in column ozone trends derived from (a) the vertically integrated SAGE/sonde data set and (b) merged TOMS/SBUV data. Trends are expressed in terms of net ozone changes (DU) over 1979–2005. Contours are −4, −8, −12, −16, −20, −30, −40, ... DU.

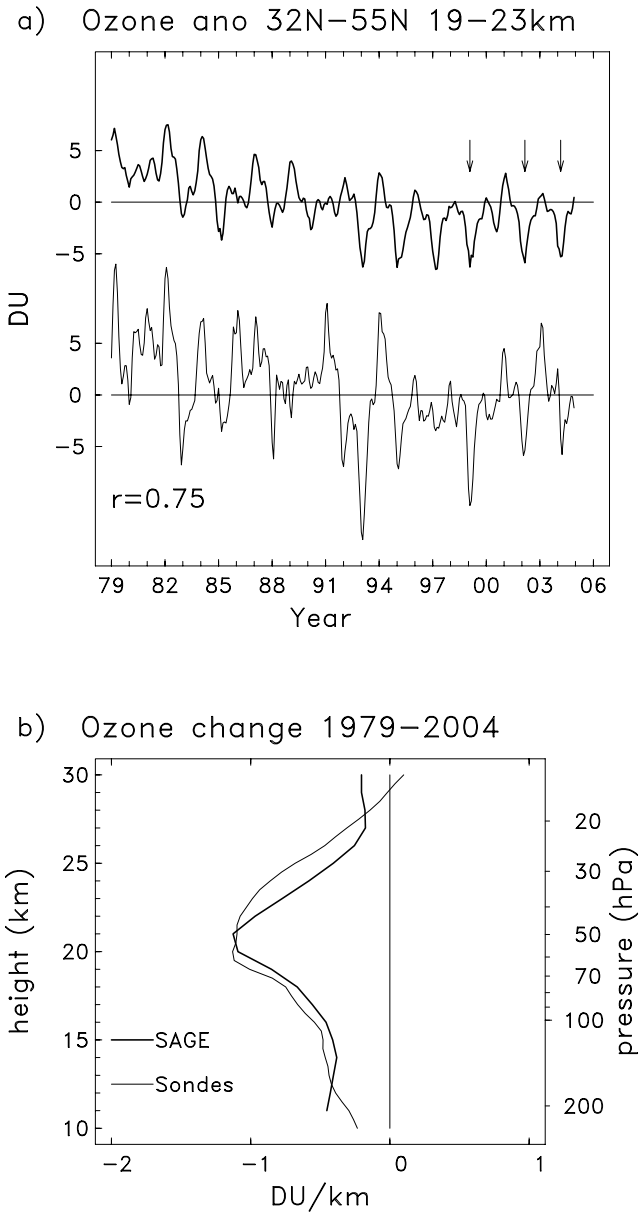

Figure 11. (a) Time series of deseasonalized ozone anomalies over NH midlatitudes (30°–55°N) in the lower stratosphere (19–23 km), derived from the SAGE profile data set (top curve) and averaged ozonesondes (bottom curve). Arrows highlight a few extrema of the QBO corresponding to the black dots in Figure 15. (b) Vertical profile of ozone trends over NH midlatitudes derived from the SAGE profile ozone data and averaged ozonesondes. Trend results are derived from regression onto the EESC trend proxy and are expressed in terms of net changes over 1979–2004 (here in units of ozone density, DU/km). Two sigma statistical uncertainty levels are of order ±0.5 DU/km throughout the profile for both data sets.

over altitudes ~15–30 km. The most simple and direct comparisons are between the SAGE data (representative of zonal means) averaged over 35°–55°N and results from the average of the 12 ozonesonde stations in Japan, Europe and North America (covering latitudes 32°–53°N; see section 2c). Figure 11a shows time series of ozone anomalies in the lower stratosphere (19–23 km) from the SAGE and ozonesonde data; note that the ozonesonde data contain the full deseasonalized variability, in contrast to the regression fit of the SAGE results. There is good overall agreement between the data sets (correlation $r = 0.75$), both in terms of overall interannual variability (dominated by the QBO) and long-term changes. The vertical profile of trends derived from the two data sets is shown in Figure 11b (expressed in terms of ozone density rather than percent, in order to show contributions to the column). The trends show exceptionally good agreement both in terms of magnitude and shape of the profile, with maximum trends near 20 km. The overall agreement with ozonesondes provides validation for the detailed variability in the SAGE data set, at least for the NH lower stratosphere.

3.4. Solar and QBO Variability

[29] The other components of variability modeled in the regression fit for SAGE data are the solar cycle and QBO terms, which are examined further here. Figure 12a shows a meridional section of the solar cycle fit to the SAGE I and II data (for 55°N–S). As noted above, we do not include a solar term in the regression below 20 km, because results based on only SAGE II data (1984–2005) show negative values, which are discontinuous from the results above 20 km and appear unrealistic. The solar fit in Figure 12a shows positive values of ~2% per 100 units $F_{10.7}$ in the middle and upper stratosphere, with a relative minimum near the equator, and a larger region of coherence in the NH midlatitudes (the values in Figure 12a should be multiplied by ~1.25 to estimate differences between solar maximum and solar minimum). The magnitude of this signal is consistent with idealized models of the ozone solar cycle [e.g., *Brasseur*, 1993; *Lee and Smith*, 2003; *Tourpali et al.*, 2003; *Egorova et al.*, 2004], although the spatial structure in Figure 12a (especially the tropical minimum) is more complicated than the relatively "flat" latitudinal structure calculated in such models. However, interpretation of the detailed structure in Figure 12a should be considered in light of the relatively short time sample of less than 3 complete solar cycles, gaps in the SAGE record, and the size of the solar effect in comparison to other variability. *Lee and Smith* [2003] suggest substantial aliasing of the solar signal in the short SAGE record, especially in the tropics, due to a combination of volcanic and QBO effects. There is some suggestion of a coherent solar signal in the lower stratosphere in Figure 12a, and a similar feature is inferred from analysis of SBUV data [*Hood*, 2004]. *Hood and Soukharev* [2003] have suggested that such a lower stratospheric signal could arise from dynamical effects.

[30] The vertically integrated solar cycle derived from SAGE I and II above 20 km is shown in Figure 12b, together with the corresponding result from the merged TOMS/SBUV column ozone data set (with statistical uncertainties). Figure 12b also includes the solar cycle regression results from two other column ozone data sets described by *Fioletov et al.* [2002] and *WMO* [2003], namely ground-based and SBUV data sets (results provided by V. Fioletov, personal communication, 2006). Overall there are substantial differences in magnitude of the solar regression coefficient between the three column ozone data sets, although

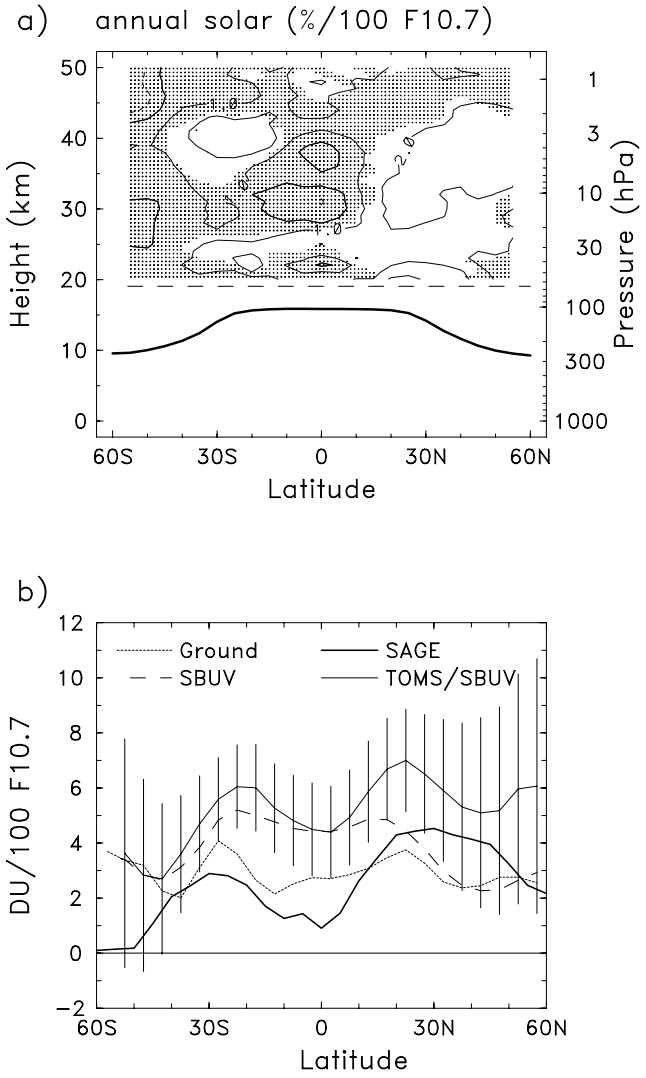

Figure 12. (a) Meridional cross section of solar cycle regression fit of the SAGE I and II data, expressed in terms of local percent per 100 units of $F_{10.7}$ radio flux (Figure 2b). Results are only calculated above 20 km, where both SAGE I and II data are available. Shading denotes that the fit is not statistically significant. (b) Latitudinal profile of the solar cycle variations in column ozone, derived from vertically integrated SAGE I and II data (over 20–50 km), and three column ozone data sets (ground-based, SBUV, and merged TOMS/SBUV data). Error bars on the TOMS/SBUV curve denote 2*sigma uncertainty in the fit.

the statistical uncertainties are also large. Comparison with the vertically integrated SAGE I and II results shows reasonable agreement with the ground-based column ozone data, whereas the SAGE results are substantially smaller than the merged TOMS/SBUV and SBUV column results (particularly over tropical latitudes). The differences could be reconciled by an additional solar component in profile ozone below 20 km. Note that *Chandra et al.* [1999] have deduced a solar signal in tropical tropospheric ozone, but that variation is out of phase with the stratospheric signal (i.e., of the wrong sign to account for the differences in Figure 12b). Overall, given the uncertainties between results from the three column ozone data sets, it is difficult to critically evaluate the solar cycle derived from the integrated SAGE results.

[31] Both the trend and solar cycle effects are relatively large in the upper stratosphere, and the combined effects produce a stair-step sequence of ozone change, with relatively flat behavior over the past decade. This is illustrated in Figure 13, showing the annual mean SAGE I and II observations at 35–45 km over 30°–55°N, together with the regression fit. This time series is similar to that observed throughout the upper stratosphere in several ozone data sets [*Steinbrecht et al.*, 2006].

[32] The QBO contributes a relatively large fraction of ozone variability over the globe, and the long record of SAGE I and II provide observations over ~10 cycles. Figure 14 shows the structure of the SAGE I and II ozone projections onto the two QBO basis functions, with results shown as local percent anomalies per standard deviation of the respective QBO time series. Because the QBO fits over extratropics are strongly seasonally dependent (maxima in winter-spring in both hemispheres), Figure 14 shows results for January–March and July–September for each of the two functions. The QBO variations are relatively large, with amplitudes of ~5–10% local background levels in both the tropics and midlatitudes (see for example the time series in Figures 3 and 11a). Spatial patterns show out-of-phase variations between the tropics and midlatitudes, with the midlatitude maxima occurring preferentially in the winter hemisphere. The observed two-cell vertical structure is related to dynamical and chemical effects in the lower and middle stratosphere, respectively [*Chipperfield et al.*, 1994; *Randel and Wu*, 1996]. The large midlatitude response, and its strong coupling to the seasonal cycle, is discussed by *Kinnersley* [1999] and *Jiang et al.* [2005].

[33] Time variation of the ozone QBO can be quantified by projection of the monthly SAGE I and II anomalies onto the spatial structures shown in Figure 14. This is done by multiplying the monthly SAGE anomalies at each latitude and height by the QBO1 and QBO2 spatial patterns (Figure 14) to produce a time series for each component (which are then normalized by the respective time series standard deviations). This provides a concise measure of the ozone QBO, analogous to the dynamical QBO analysis discussed by *Wallace et al.* [1993]. Figure 15 shows a "phase space" diagram of the monthly projections onto QBO1 and

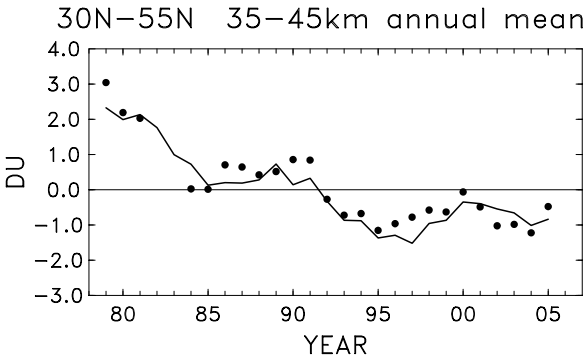

Figure 13. Time series of annual average ozone anomalies from SAGE I and II data, averaged over 35–45 km and 30°–55°N, together with the associated regression fit.

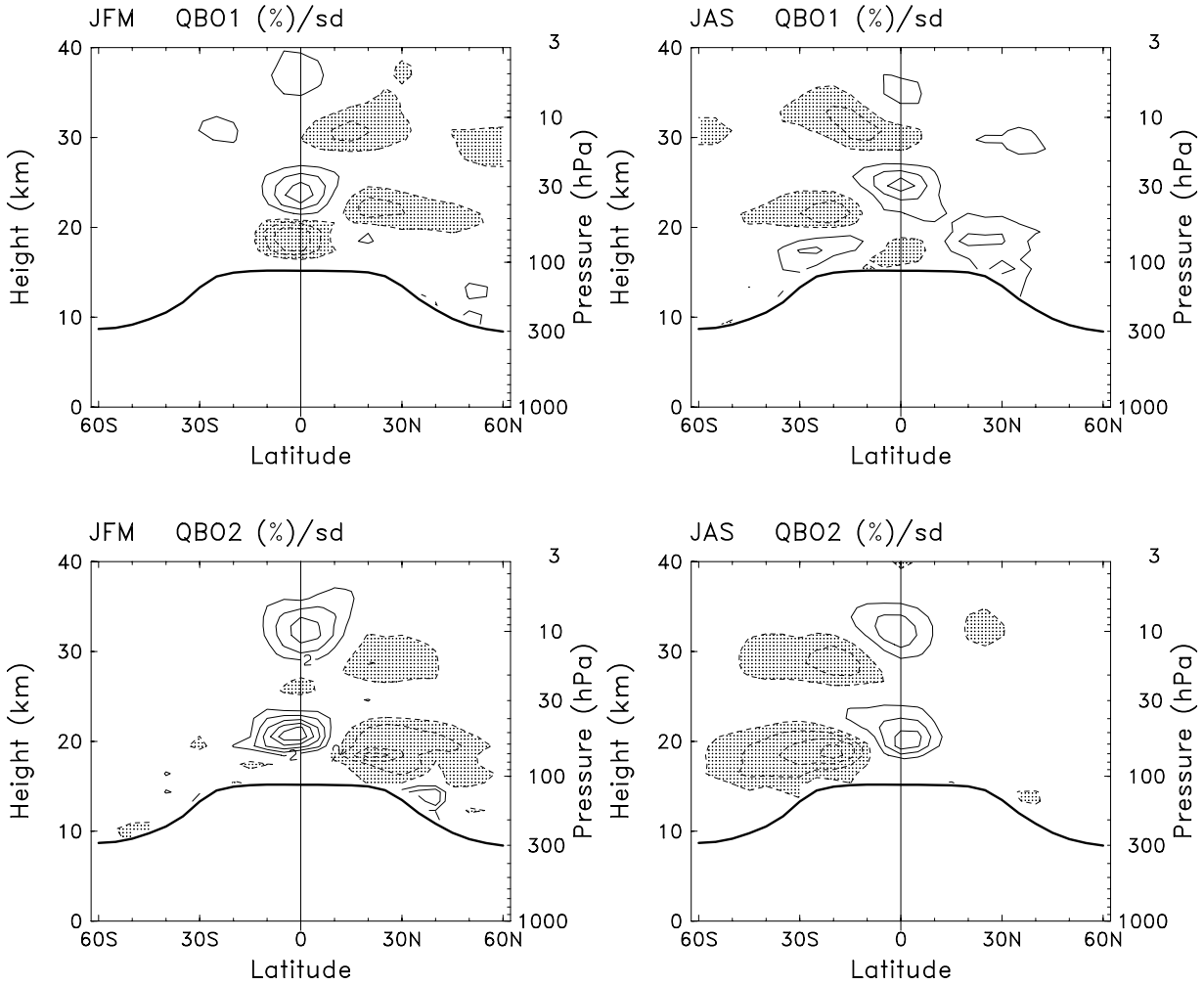

Figure 14. Meridional cross sections showing QBO spatial variations in SAGE I and II data, derived from regression onto two orthogonal QBO basis functions (shown in the top and bottom plots). Because the extratropical fits are strongly seasonally dependent, results are shown for (left) January–March and (right) July–September. Contours show local percent variations in ozone associated with one standard deviation in the respective time series, with contours of ±2, 4, 6…% (zero contours are omitted, and negative values are shaded).

QBO2 (each smoothed with a 3-month running mean); time progression corresponds to clockwise transits (or orbits of the ozone QBO), with one cycle corresponding to a QBO cycle. Figure 15 quantifies the regular appearance and phase progression of the ozone QBO through approximately ten QBO cycles during 1979–2005 (data are missing for the SAGE gaps during 1982–1984 and 1991–1993). On the basis of the spatial structures in Figure 14, large QBO anomalies in extratropics correspond to periods with same-signed projections in QBO1 and QBO2. For example, Figure 15 indicates three specific months (black dots) when this occurs (during NH winter 1998–1999, 2001–2002 and 2003–2004), and these periods correspond to large QBO anomalies over the NH indicated in the time series in Figure 11a.

4. Summary and Discussion

[34] In this work we have generated a global ozone profile data set covering the period 1979–2005, based on a combination of SAGE I and II satellite measurements and polar ozonesondes. The strengths of the SAGE data are their high data quality over time and high vertical resolution (due to the solar occultation measurement technique), and their temporal sampling is adequate for analysis of low-frequency interannual variability. The data derived here from regression analysis are intended to provide an altitude-resolved depiction of global-scale ozone variability and change, covering altitudes from the tropopause to 50 km. These data may be useful for global modeling studies, such as analysis of the stratospheric response to decadal ozone changes (they have been used for the model simulations discussed by *Ramaswamy et al.* [2006]). They also allow comparisons with other observational ozone data sets, in particular global column ozone data from satellites and ozone profiles over NH midlatitudes observed by ozonesondes. The vertically integrated SAGE/sonde data capture the majority of interannual variability observed in column ozone data, and the SAGE results also show excellent

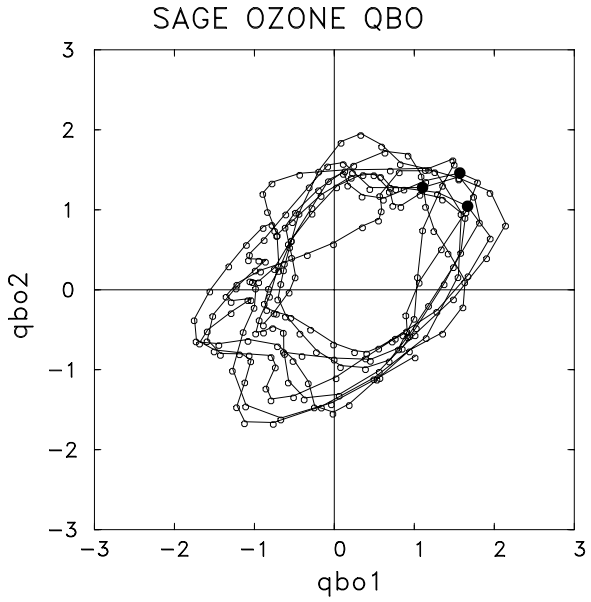

Figure 15. Phase space diagram of the global ozone QBO in SAGE I and II data. Time series of the projection of the monthly SAGE anomalies onto the QBO1 and QBO2 spatial structure functions (Figure 14) are calculated, normalized by the time series standard deviation, and each circle shows the projections for individual months during 1979–2005 (with SAGE gaps during 1982–1984 and 1991–1993). This provides a concise measure of the global coherence and phase progression of the ozone QBO. Time progression coincides with clockwise orbit transits. The black dots highlight three NH winter periods with large midlatitude QBO signals (corresponding to the arrows in Figure 11a).

agreement with ozonesondes throughout the NH lower stratosphere (Figure 11). These comparisons provide an independent check of the SAGE/sonde results (derived from regression), and allow analysis of the vertical structure of variability observed in column ozone measurements. One limitation of these data is that ozone changes associated with the Mt. Pinatubo volcanic eruption [*Tie et al.*, 1994; *Stolarski et al.*, 2006] are not resolved (because of absence of data in postvolcanic periods).

[35] The overall ozone trend results derived here are similar to previous analyses of SAGE data, with maximum trends in the upper and lower stratosphere, and a minimum near 25–30 km, and these results are in reasonable agreement with other data sources [*WMO*, 2003; *Rosenfield et al.*, 2005]. We find exceptionally good agreement between SAGE trends and results derived from a combined ozonesonde data set over NH midlatitudes (Figure 11b). SAGE data suggest relatively large (percentage) ozone decreases in the tropical lower stratosphere (Figure 8a), but the vertically integrated trends in this region are substantially larger than observed column ozone trends in the tropics (Figure 8b). These could be reconciled by corresponding increases in tropical tropospheric ozone, but the latter are poorly constrained from observations. Because the tropical lower stratosphere is a region that presents difficulty for satellite ozone measurements (low ozone amount, strong vertical gradient, and possible aerosol contamination), the SAGE results should be viewed cautiously. On the other hand, the SAGE II data show good agreement in this region with interannual changes observed in SHADOZ [*Thompson et al.*, 2003] ozonesonde data since 1998 [*Randel et al.*, 2006]. Overall this is a region of importance for ongoing research (as discussed by *Solomon et al.* [2005]).

[36] The solar signal derived from the updated SAGE data shows in-phase variations in the middle and upper stratosphere that are consistent with idealized model calculations (i.e., ~2–3% variations between solar maximum and solar minimum), but the spatial pattern derived from SAGE is more complicated than that found in models (in particular, the SAGE results show a minimum in the tropical middle stratosphere). The differences could be attributable to substantial uncertainties in the relatively short, gappy SAGE record (and the fact that the solar signal is a relatively small signal), or to effects not captured in idealized models. Additionally, there are substantial uncertainties in magnitude of the solar cycle in column ozone from different data sets (Figure 12b), so that it is difficult to critically constrain the integrated SAGE results.

[37] The QBO dominates the interannual variability in ozone over much of the globe, and the long record of high vertical resolution data from SAGE allows accurate characterization of the space-time QBO structure. Local QBO anomalies are typically 5–10% local background values (Figure 14), with a two-cell vertical structure and coherent out-of-phase behavior between the tropics and extratropics. The extratropical QBO patterns maximize in the winter hemisphere, and account for the largest anomalies observed in time series (e.g., Figures 3 and 11a). This is an aspect of global ozone variability that should be considered carefully in modeling studies or model-data comparisons.

[38] The SAGE/sonde deseasonalized anomaly data set discussed here has been combined with the global ozone climatology of *Fortuin and Kelder* [1998], to generate a full seasonally varying zonal mean ozone data set applicable for model studies. These data are available to the research community via anonymous ftp at acd.ucar.edu/user/randel/o3data.

[39] **Acknowledgments.** The parameterization for the EESC time series and the solar cycle regression results for ground-based and SBUV data sets were provided by Vitali Fioletov. We thank Vitali Fioletov and Rich Stolarski for discussions during the course of this work and Louisa Emmons and Anne Smith for comments on the manuscript. This work is partially supported under the NASA ACMAP program. The National Center for Atmospheric Research is operated by the University Corporation for Atmospheric Research under the sponsorship of the National Science Foundation.

References

Bengtsson, L., E. Roeckner, and M. Stendel (1999), Why is the global warming proceeding much slower than expected?, *J. Geophys. Res.*, *104*, 3865–3876.

Bortz, S. E., M. J. Prather, J.-P. Cammas, V. Thouret, and H. Smit (2006), Ozone, water vapor, and temperature in the upper tropical troposphere: Variations over a decade of MOZAIC measurements, *J. Geophys. Res.*, *111*, D05305, doi:10.1029/2005JD006512.

Brasseur, G. (1993), The response of the middle atmosphere to long-term and short-term solar variability: A two-dimensional model, *J. Geophys. Res.*, *98*, 23,079–23,090.

Chandra, S., J. R. Ziemke, and R. W. Stewart (1999), An 11-year solar cycle in tropospheric ozone from TOMS measurements, *Geophys. Res. Lett.*, *26*, 185–188.

Chipperfield, M. P., L. J. Gray, J. S. Kinnersley, and J. Zarodny (1994), A two-dimensional model study of the QBO signal in SAGE II NO_2 and O_3, *Geophys. Res. Lett.*, *21*, 589–592.

Dameris, M., et al. (2005), Long-term changes and variability in a transient simulation with a chemistry-climate model employing realistic forcing, *Atmos. Chem. Phys.*, *5*, 2121–2145.

Egorova, T., E. Rozanov, E. Manzini, M. Haberreiter, W. Schmutz, V. Zubov, and T. Peter (2004), Chemical and dynamical response to the 11-year variability of the solar irradiance simulated with a chemistry-climate model, *Geophys. Res. Lett.*, *31*, L06119, doi:10.1029/2003GL019294.

Fioletov, V. E., and T. G. Shepherd (2005), Summertime total ozone variations over middle and polar latitudes, *Geophys. Res. Lett.*, *32*, L04807, doi:10.1029/2004GL022080.

Fioletov, V. E., G. E. Bodeker, A. J. Miller, R. D. McPeters, and R. Stolarski (2002), Global and zonal total ozone variations estimated from ground-based and satellite measurements: 1964–2000, *J. Geophys. Res.*, *107*(D22), 4647, doi:10.1029/2001JD001350.

Fortuin, J. P. F., and H. Kelder (1998), An ozone climatology based on ozonesonde and satellite measurements, *J. Geophys. Res.*, *103*, 31,709–31,734.

Hadjinicolaou, P., J. A. Pyle, M. P. Chipperfield, and J. A. Kettleborough (1997), Effect of interannual meteorological variability on mid-latitude O_3, *Geophys. Res. Lett.*, *24*, 2993–2996.

Hood, L. L. (2004), Effects of solar UV variability on the stratosphere, in *Solar Variability and Its Effects on Climate*, *Geophys. Monogr. Ser.*, vol. 141, edited by J. Pap and P. Fox, pp. 283–304, AGU, Washington, D. C.

Hood, L., and B. Soukharev (2003), Quasi-decadal variability of the lower stratosphere: The role of extratropical wave forcing, *J. Atmos. Sci.*, *60*, 2389–2403.

Jiang, X., D. B. A. Jones, R. Shia, D. E. Waliser, and Y. L. Yung (2005), Spatial patterns and mechanisms of the quasi-biennial oscillation—Annual beat of ozone, *J. Geophys. Res.*, *110*, D23308, doi:10.1029/2005JD006055.

Kinnersley, J. S. (1999), Seasonal asymmetry of the low- and middle-latitude QBO circulation anomaly, *J. Atmos. Sci.*, *56*, 1140–1153.

Langematz, U., M. Kunze, K. Krüger, K. Labitzke, and G. L. Roff (2003), Thermal and dynamical changes of the stratosphere since 1979 and their link to ozone and CO_2 changes, *J. Geophys. Res.*, *108*(D1), 4027, doi:10.1029/2002JD002069.

Lee, H., and A. K. Smith (2003), Simulation of the combined effects of solar cycle, quasi-biennial oscillation and volcanic forcing on stratospheric ozone changes in recent decades, *J. Geophys. Res.*, *108*(D2), 4049, doi:10.1029/2001JD001503.

Lelieveld, J., J. van Aardenne, H. Fischer, M. de Reus, J. Williams, and P. Winkler (2004), Increasing ozone over the Atlantic Ocean, *Science*, *304*, 1483–1487.

Li, J., D. M. Cunnold, H.-J. Wang, E.-S. Yang, and M. J. Newchurch (2002), A discussion of upper stratospheric ozone asymmetries and SAGE trends, *J. Geophys. Res.*, *107*(D23), 4705, doi:10.1029/2001JD001398.

Logan, J. A., et al. (1999), Trends in the vertical distribution of ozone: A comparison of two analyses of ozonesonde data, *J. Geophys. Res.*, *104*, 26,373–26,400.

McCormick, M. P., J. M. Zawodny, R. E. Viega, J. C. Larson, and P. H. Wang (1989), An overview of SAGE I and II ozone measurements, *Planet. Space Sci.*, *37*, 1567–1586.

Newchurch, M. J., M. A. Ayoub, S. Oltmans, B. Johnson, and F. J. Schmidlin (2003), Vertical distribution of ozone at four sites in the United States, *J. Geophys. Res.*, *108*(D1), 4031, doi:10.1029/2002JD002059.

Ramaswamy, V., M. D. Schwarzkopf, W. J. Randel, B. D. Santer, B. J. Soden, and G. Stenchikov (2006), Anthropogenic and natural influences in the evolution of lower stratospheric cooling, *Science*, *311*, 1138–1141.

Randel, W. J., and F. Wu (1996), Isolation of the ozone QBO in SAGE II data by singular value decomposition, *J. Atmos. Sci.*, *53*, 2546–2559.

Randel, W. J., and F. Wu (1999), A stratospheric ozone trends data set for global modeling studies, *Geophys. Res. Lett.*, *26*, 3089–3092.

Randel, W. J., F. Wu, H. Vömel, G. E. Nedoluha, and P. Forster (2006), Decreases in stratospheric water vapor after 2001: Links to changes in the tropical tropopause and the Brewer-Dobson circulation, *J. Geophys. Res.*, *111*, D12312, doi:10.1029/2005JD006744.

Rosenfield, J. E., S. M. Frith, and R. S. Stolarski (2005), Version 8 SBUV ozone profile trends compared with trends from a zonally averaged chemical model, *J. Geophys. Res.*, *110*, D12302, doi:10.1029/2004JD005466.

Santer, B. D., et al. (1996), A search for human influences on the thermal structure of the atmosphere, *Nature*, *382*, 9–46.

Shine, K. P., et al. (2003), A comparison of model-simulated trends in stratospheric temperatures, *Q. J. R. Meteorol. Soc.*, *129*, 1565–1588.

Solomon, S., D. W. J. Thompson, R. W. Portmann, S. J. Oltmans, and A. M. Thompson (2005), On the distribution and variability of ozone in the tropical upper troposphere: Implications for tropical deep convection and chemical-dynamical coupling, *Geophys. Res. Lett.*, *32*, L23813, doi:10.1029/2005GL024323.

Steinbrecht, W., et al. (2006), Long-term evolution of upper stratospheric ozone at selected stations of the Network for the Detection of Stratospheric Change (NDSC), *J. Geophys. Res.*, *111*, D10308, doi:10.1029/2005JD006454.

Stolarski, R. S., A. R. Douglass, S. Steenrod, and S. Pawson (2006), Trends in stratospheric ozone: Lessons learned from a 3D chemical transport model, *J. Atmos. Sci.*, *63*, 1028–1041.

Stratospheric Processes and their Role in Climate (1998), SPARC/IOC/GAW assessment of trends in the vertical distribution of ozone, *SPARC Rep. 1*, edited by N. Harris et al., 289 pp., Verrieres le Buisson, France.

Thompson, A. M., et al. (2003), Southern Hemisphere Additional Ozonesondes (SHADOZ) 1998–2000 tropical ozone climatology: 1. Comparison with Total Ozone Mapping Spectrometer (TOMS) and ground-based measurements, *J. Geophys. Res.*, *108*(D2), 8238, doi:10.1029/2001JD000967.

Tie, X. X., C. Granier, W. Randel, and G. Brasseur (1994), Two-dimensional model simulation of Pinatubo aerosol and its effect on stratospheric ozone, *J. Geophys. Res.*, *99*, 20,545–20,562.

Tourpali, K., C. J. E. Schuurmans, R. van Dorland, B. Steil, and C. Brühl (2003), Stratospheric and tropospheric response to enhanced solar UV radiation: A model study, *Geophys. Res. Lett.*, *30*(5), 1231, doi:10.1029/2002GL016650.

Wallace, J. M., R. L. Panetta, and J. Estberg (1993), Representation of the equatorial quasi-biennial oscillation in EOF phase space, *J. Atmos. Sci.*, *50*, 1751–1762.

Wang, H. J., D. M. Cunnold, and X. Bao (1996), A critical assessment of Stratospheric Aerosol and Gas Experiment ozone trends, *J. Geophys. Res.*, *101*, 12,495–12,514.

Wang, H. J., D. M. Cunnold, L. W. Thomason, J. M. Zawodny, and G. E. Bodeker (2002), Assessment of SAGE version 6.1 ozone data quality, *J. Geophys. Res.*, *107*(D23), 4691, doi:10.1029/2002JD002418.

World Meteorological Organization (WMO) (2003), Scientific assessment of ozone depletion: 2002, *Global Ozone Res. Monit. Proj. Rep. 47*, Geneva, Switzerland.

Ziemke, J. R., S. Chandra, and P. K. Bhartia (2005), A 25-year data record of atmospheric ozone in the Pacific from Total Ozone Mapping Spectrometer (TOMS) cloud slicing: Implications for ozone trends in the stratosphere and troposphere, *J. Geophys. Res.*, *110*, D15105, doi:10.1029/2004JD005687.

W. J. Randel and F. Wu, National Center for Atmospheric Research, Boulder, CO 80307, USA. (randel@ucar.edu)